JOBNAME: JCLI 00#0 2011 PAGE: 1 SESS: 8 OUTPUT: Tue Mar 8 11:16:07 2011 Total No. of Pages: 12
/ams/jcli/0/jcli4069

Journal of Climate (Proof Only)

Northern Hemisphere Modes of Variability and the Timing of Spring in Western North America

TOBY R. AULT AND ALISON K. MACALADY

University of Arizona, Tucson, Arizona

GREGORY T. PEDERSON

U. S. Geological Survey, Bozeman, Montana

JULIO L. BETANCOURT

U. S. Geological Survey, Tucson, Arizona

MARK D. SCHWARTZ

University of Wisconsin—Milwaukee, Milwaukee, Wisconsin

(Manuscript received 10 September 2010, in final form 28 January 2011)

ABSTRACT

Spatial and temporal patterns of variability in spring onset are identified across western North America using a spring index (SI) model based on weather station minimum and maximum temperatures (T_{min} and T_{max}, respectively). Principal component analysis shows that two significant and independent patterns explain roughly half of the total variance in the timing of spring onset from 1920 to 2005. However, these patterns of spring onset do not appear to be linear responses to the primary modes of variability in the Northern Hemisphere: the Pacific–North American pattern (PNA) and the northern annular mode (NAM). Instead, over the period when reanalysis data and the spring index model overlap (1950–2005), the patterns of spring onset are local responses to the state of both the PNA and NAM, which together modulate the onset date of spring by 10–20 days on interannual time scales. They do so by controlling the number and intensity of warm days. There is also a regionwide trend in spring advancement of about −1.5 days decade^{-1} from 1950 to 2005. Trends in the NAM and PNA can only explain about one-third (−0.5 day decade^{-1}) of this trend.

1. Introduction

Spring is marked by dramatic phenological events: plants put on leaves and flowers, animals migrate, insects emerge, and the whole Northern Hemisphere becomes visibly greener from space. A sequence of temperature and precipitation fluctuations influence the timing of certain phenological events, which in turn cascade through ecosystems and feed back to the atmosphere via carbon and water cycling (Schwartz 1992). Both phenoclimatic indicators (indices based on weather) and actual phenological observations (e.g., the first appearance of leaves or flowers) are synchronized and generally covary from year-to-year at regional scales (Cayan et al. 2001; Schwartz et al. 2006). This implies that the sequence of temperature and precipitation fluctuations that trigger spring onset in the biological world may be organized by certain modes of climate variability. If the state of these modes can be anticipated on seasonal-to-interannual and decadal time scales, then the dates of spring onset might be predictable and could be used to manage natural resources and mitigate natural hazards. For instance, spring onset is associated with variability in streamflow, drought, wildfire activity, and the timing and yield of agricultural crops (Betancourt et al. 2005). Forecasts of spring onset with seasonal or annual lead times could help farmers optimize planting and irrigating schedules, water managers anticipate delivery shortages, and foresters allocate resources for fighting fires or managing insect outbreaks. In addition, improved ecological understanding and advance

Corresponding author address: Toby R. Ault, Dept. of Geosciences, University of Arizona, 1040 E. 4th St., Tucson, AZ, 85701.
E-mail: tault@email.arizona.edu

DOI: 10.1175/2011JCLI4069.1

© 2011 American Meteorological Society

JOBNAME: JCLI 00#0 2011 PAGE: 2 SESS: 8 OUTPUT: Tue Mar 8 11:16:07 2011 Total No. of Pages: 12
/ams/jcli/0/jcli4069

Journal of Climate (Proof Only)

knowledge of how spring onset is likely to vary on decadal time scales could guide strategic investments in invasive species removal, forest harvesting and replanting, and assisted migration.

Here, we investigate the role of dominant modes of atmospheric variability in modulating spatial and temporal variability in spring onset across western North America (WNA) over the past century. More specifically, we use phenological models of lilac and honeysuckle, based on daily minimum and maximum temperatures (T_{min} and T_{max}, respectively), to develop indices for the onset of spring (Schwartz et al. 2006), identify spatial and temporal patterns of variability in those indices, and examine atmospheric controls on the temperature fluctuations that control them.

The magnitude and rate of climatic warming across WNA outpaced the global average during the second-half of the twentieth century (Solomon et al. 2007; Karl et al. 2009; Bonfils et al. 2008). Warming has been especially pronounced during spring, with March–May (MAM) temperatures rising 0.36°C decade^{-1}, almost twice the annual rate (Abatzoglou and Redmond 2007). Spring warming in WNA has been implicated in dramatic changes to plant and animal phenologies (Inouye 2008; Forister and Shapiro 2003; Cayan et al. 2001; Schwartz and Reiter 2000; Brown et al. 1999; Caprio 1993), changes in snowpack, snowmelt and associated streamflow (Mote et al. 2005; Stewart et al. 2005; McCabe and Clark 2005; Hamlet et al. 2007; Barnett et al. 2008; Pierce et al. 2008; Hidalgo et al. 2009; Das et al. 2009), glacier recession (Moore et al. 2009), and enhanced wildfire activity (McKenzie et al. 2004; Westerling et al. 2006; Littell et al. 2009). These findings raise the possibility that forced changes in circulation, as well as radiative changes, may be pacing the trends in phenology and hydrology.

Large-scale patterns of atmospheric circulation are important drivers of interannual variability in winter climate across the Northern Hemisphere (Thompson and Wallace 2000; Quadrelli and Wallace 2004) and have been linked to variability in plant phenology and peak runoff in the western United States and Eurasia (Cayan et al. 2001; Stenseth et al. 2002; Johnson et al. 2007; de Beurs and Henebry 2008). We focus on two modes of Northern Hemisphere variability to aid our interpretation of temporal and regional variability in spring onset. These are the Pacific–North American pattern (PNA) and the northern annular mode (NAM), which are particularly dominant in the Northern Hemisphere winter and spring, and which together explain 30% of all variance in monthly sea level pressure (Quadrelli and Wallace 2004). Although defined at the monthly time scale, these modes also exhibit energetic fluctuations at higher frequencies (Thompson and Wallace 2001). The PNA is characterized by a deepened Aleutian low and enhanced ridge over British Columbia, Canada, during its positive phase (Wallace and Gutzler 1981). Under this configuration, spring temperatures tend to be warmer than average across much of the U.S. Pacific Northwest and western Canada and cooler than average in the U.S. Southwest and Southeast. This mode is strongly influenced by variability in the Tropical and North Pacific and is associated with El Niño–Southern Oscillation (ENSO) and the Pacific decadal oscillation (PDO); the positive phase of either ENSO or the PDO favors a positive phase of the PNA (e.g., Zhang et al. 1997) and warmer spring. The NAM is a planetary-scale wave with a trough over the North Pole and relative highs over the northern Atlantic and Pacific Oceans during its positive phase (these relative highs and lows have the opposite polarity during the NAM's negative phase) (Thompson and Wallace 2000). It influences the position of storm tracks in the Northern Hemisphere and the number and intensity of midlatitude cold outbreaks in winter (Thompson and Wallace 2001; McAfee and Russell 2008). During its positive phase, the jet stream in North America tends to be displaced to the north and flow tends to be more zonal. The negative phase, in contrast, is associated with a southward position of the jet, enhanced meridional flow, and a greater number of cold outbreaks across North America.

To evaluate the role of climate variability in modulating spring arrival, we use spring indices (SIs) because they offer certain advantages over direct phenological measurements and other types of proxies for spring onset. First, the phenology of cloned lilac and honeysuckle has been extensively monitored since the 1950s and is "well behaved" in the sense that these plants respond directly to changes in temperature as opposed to changes in day length or other environmental cues (Caprio 1993). These characteristics allowed for the development of a numerical model of phenology that is well validated and that can be calculated wherever climate information is available but phenological observations are not (Schwartz and Marotz 1986, 1988). Second, SI can be computed from daily temperature records anywhere where sufficient chilling is achieved during the winter and where sufficient warmth is achieved during the summer. In contrast, hydrologic metrics, such as snow water equivalent, center of timing, and center of mass, are inherently biased toward changes occurring at high elevations where snow accumulates with regularity. Third, the model has been validated against lilacs and selected native species in a variety of climates and geographies on several continents, and it has consistently been shown to be a reliable metric of the plant-level response to spring warming (Schwartz and Marotz 1986, 1988; Schwartz et al. 1997;

JOBNAME: JCLI 00#0 2011 PAGE: 3 SESS: 8 OUTPUT: Tue Mar 8 11:16:07 2011 Total No. of Pages: 12
/ams/jcli/0/jcli4069

Journal of Climate (Proof Only)

Schwartz and Reiter 2000; Schwartz et al. 2006). Lastly, spring indices are calculated from temperature records alone, which isolate the thermal component of spring onset. Direct phenological observations, in contrast, may be influenced by a wider range of climate variables (e.g., snow, precipitation, and cloudiness).

2. The spring index model

We identify the onset of spring using a synoptic model of phenology initially developed by Schwartz and Marotz (1986, 1988), then subsequently improved by Schwartz et al. (1997, 2006). The model is constructed to translate noisy temperature fluctuations into an index of the timing of spring, much in the same way that drought indices translate hydroclimatic fluctuations into time series of anomalously wet or dry conditions (e.g., Palmer 1965; Alley 1984; Guttman 1999). In effect, this approach provides us with a definition of spring onset that is consistent across space and through time.

Suppose that a "phenological event" (e.g., the appearance of the first leaves) occurs when a plant detects the transition from winter to spring from some discrete set of physical variables (e.g., temperature, day length, humidity). If the phenological event is linearly related to the physical variables, it could be modeled from a set of predictors such that

$$\frac{1}{Y} = C_0 + \sum_{i=1}^{N} \frac{X_i C_i}{Y}, \qquad (1)$$

where Y is the date of the phenological event, $X_{1,2,\ldots N}$ are the independent predictor variables, $C_{1,2,\ldots N}$ are regression coefficients, and C_0 is the regression constant. This formulation ensures that different dates for the same event across stations or years do not bias the regression (Schwartz 1985).

This framework has been used to model the phenology of three plant species, for which extensive observations are available (Caprio 1993), and has been widely tested throughout the world (Schwartz et al. 2006). These plants are common lilac *Syringa chinensis* "Red Rothomagensis" or cloned lilac, and two cloned honeysuckles: *Lonicera tatarica*, "Arnold Red" and *L. korolkowii* "Zabeli."

A set of metrics, called the "spring indices suite of measures," were used in earlier studies (Schwartz et al. 2006; Schwartz and Chen 2002; Schwartz and Reiter 2000) by averaging together the phenological events of the three plant species. Here, we restrict our analysis to the "first leaf" index, although results were similar for analyses on the "first bloom" index. The first leaf index is an important marker of the beginning of spring because once plants have started putting on summer foliage, there is a measurable influence on the atmosphere (Schwartz and Karl 1990; Schwartz 1992). Herein we use "the timing of spring" and "spring onset date" interchangeably to refer to the leaf index. Figure 1 shows the long-term mean calendar day of the leaf index for each record used here.

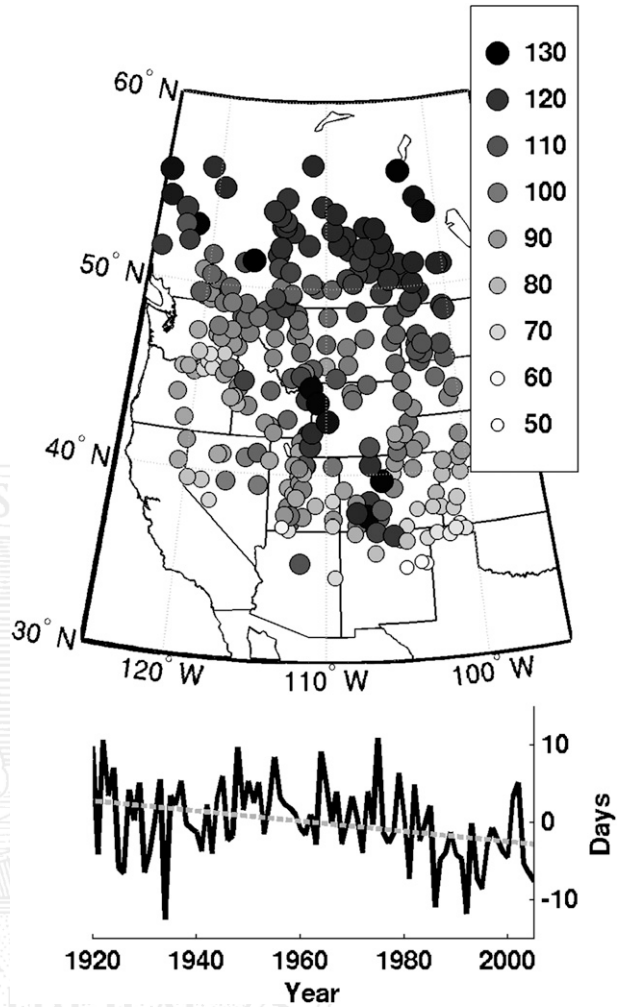

FIG. 1. Mean leaf index value (days from start of year) for stations in WNA. Day 60 corresponds to 1 Mar, day 90 corresponds to 31 Mar, and day 120 corresponds to 30 Apr.

The predictor variables X_i in the leaf index model are as follows: 1) the number of warm events; 2) accumulated growing degree hours (AGDH) during the last 3 days; 3) AGDH 5–7 days earlier; and 4) the calendar date. It is worth emphasizing that the model regression coefficients remain the same regardless of longitude, elevation, and other site-specific characteristics, which ensures that the model represents the same event across different climates. Also note that all predictors increase with time during spring, so that multiplying Eq. (1) by Y sets up an inequality if the phenological event has not yet occurred:

JOBNAME: JCLI 00#0 2011 PAGE: 4 SESS: 8 OUTPUT: Tue Mar 8 11:16:09 2011 Total No. of Pages: 12
/ams/jcli/0/jcli4069

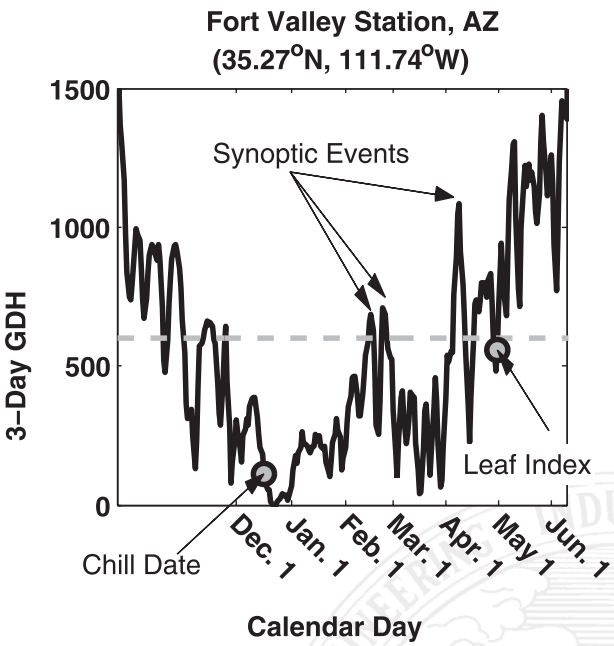

FIG. 2. Diagram of cumulative 3-day AGDH totals from one station during winter and spring of one year (1991/1992). The first dot indicates when the chilling requirements were met during fall of the antecedent year (16 Dec 1991). After this point, the model starts recording spring time warming, which first occurs when air masses are advected to the station from the south. These pulses of warmth can be seen as rapid increases in AGDH. If these events are sufficiently warm (i.e., above the gray dotted line), they are recorded as synoptic events, which are used as predictor variables in the model (Schwartz and Marotz 1986). The next dot indicates the day that the model predicts first leaf (29 Apr 1992).

$$1 > YC_0 + \sum_{i=1}^{N} X_i C_i. \qquad (2)$$

The model therefore simply calculates all predictor variables at each (daily) time step for each plant and tests if Eq. (2) is still valid. If the inequality is still valid, the model moves on to the next day and repeats the calculations. If it is not valid, then sufficient heat has accumulated for leafout to occur, and the day when this happens is recorded.

F2 Figure 2 illustrates how the SI model works using a time series of 3-day growing degree hour accumulations for one cold season (1991/92). First, the model tallies up chilling hours (e.g., hours spent below a threshold of −2.2°C) until the requirements of each plant species are met (1350 h for lilac and 1250 h for the two varieties of honeysuckle). After the chilling requirements have been satisfied (the first gray dot in Fig. 2), the model starts recording the accumulation of recent growing-degree hours and the number of "high-energy synoptic events" (defined in Schwartz and Marotz 1988 as the accumulation of 600 AGDH in 3 days). These are periods of time when temperatures rise very quickly for several days, usually through the advection of warm air masses from the south (Schwartz and Marotz 1986, 1988). Several such pulses can be seen as spikes in the time series of 3-day ADGH in Fig. 2. At each (daily) time step, the model checks if the requirements are met, at which point the event is assumed to have occurred.

3. Data and methods

We used daily T_{min} and T_{max} from records in the National Climatic Data Center (NCDC) database to compute indices. Details of the station data used in this analysis are provided in Schwartz et al. (2006). Briefly, these are U.S. Historical Climate Network (HCN) stations that were included if they experienced sufficient chilling during the winter (and warming during the spring and summer) to make the computation valid during at least 25 out of the 30 yr between 1960 and 1991. Further, individual years were only included if they did not have any intervals with missing values exceeding 10 days in any 30-day period over the entire year. Indices were computed from records of T_{min} and T_{max} at 265 stations across WNA (35°–55°N and west of 100°W). We also generated a gridded version of the dataset by averaging the leaf index to an evenly spaced 5° by 5° grid to remove the potential for regional biases that might arise from variable station densities.

In addition to the station data, we use several observational datasets to examine the large-scale atmospheric controls on the timing of spring:

(i) Principal component time series of NAM and PNA from the University of Washington's Joint Institute for the Study of the Atmosphere and Ocean (JISAO). These time series were computed by performing principal component analysis on the anomalous monthly National Centers for Environmental Prediction (NCEP) sea level pressure field north of 20°N.
(ii) Monthly 300-mb-height fields obtained from the NCEP reanalysis project (Kalnay et al. 1996). In this product, pressure surfaces are integrated on a 2.5° × 2.5° grid using assimilated observations from 1949 onward.
(iii) Daily surface T_{min} and T_{max} fields from NCEP reanalysis data. Since there are well-known biases in the NCEP surface data (e.g., Qian et al. 2006), these fields are only used to estimate the number of high-energy synoptic events (e.g., the rapid accumulation of growing degree days defined by Schwartz and Marotz 1988) during spring.

Journal of Climate (Proof Only)

JOBNAME: JCLI 00#0 2011 PAGE: 5 SESS: 8 OUTPUT: Tue Mar 8 11:16:09 2011 Total No. of Pages: 12
/ams/jcli/0/jcli4069

Journal of Climate (Proof Only)

We estimated magnitude of the leaf index trend as the slope of a least squares regression line over the time period from 1950 to 2005. Trends were estimated from raw leaf index data across the entire domain and from the time series of the gridded leaf index. We also estimated the slope of the trend from 1950 to 2005 after removing the influences of the PNA and NAM. We did so by using the PNA and NAM as predictor variables in a linear least squares regression model of the regionwide leaf index average, then calculating the slope of the residual trend (i.e., the trend of the leaf index average not explained by regression model).

To identify large-scale patterns of covariability in the leaf index, we performed principal component analysis on the 265 WNA leaf index time series. Raw eigenvectors were derived from the covariance matrix estimated from 1920 to 2005, orthogonally rotated (using the varimax criterion) and projected onto the original data to produce principal component time series (rPCs). These rPCs were then normalized to unit variance and regressed against the original data so that the spatial coefficients of the leading patterns correspond to days of change in the leaf index per one standard deviation in the corresponding rPC. Significance of the leading rPCs was determined using the Rule-N criterion (Preisendorfer et al. 1988).

The leading two rPC time series were correlated with surface temperature and 300-mb-height fields. We also regressed the time series of the PNA and NAM against each point in the gridded version of the leaf index. Since the NAM and PNA are the leading patterns of covariability in the atmosphere, and are by construction orthogonal, we show these regression slopes as vectors using a similar technique described by Quadrelli and Wallace (2004). Specifically, the number of days of change in the leaf index per one standard deviation of change in the NAM is shown along the x axis, and the PNA regression slope is shown along the y axis.

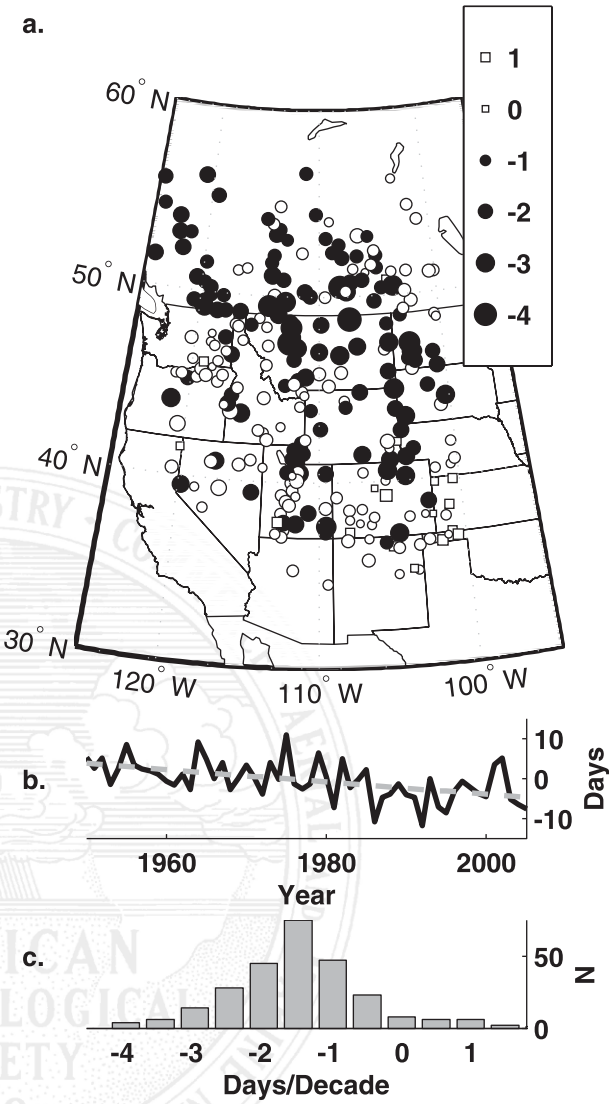

FIG. 3. (a) Map of trends in the leaf index calculated from western stations: size indicates magnitude (days decade^{-1}), shading indicates that the trend was significantly different from zero at the 95% confidence level. (b) Time series of the mean leaf index date for the entire domain. Stations were averaged to a 5° × 5° grid prior to calculating the average. (c) Distribution of trends (days decade^{-1}) from all stations.

4. Results

Trends in leaf index are negative (i.e., toward earlier spring) where they are significant (Fig. 3a). The subcontinental trend is about −1.5 days decade^{-1} from 1950 to 2005 (Fig. 3b), with most of the sites experiencing an advancement of spring by about −0.5 to −2.5 days decade^{-1} (Fig. 3c). Approximately one-third of the trend in the mean leaf index time series can be explained by trends in the PNA and NAM (−0.5 day decade^{-1}). The remaining trend (−1 day decade^{-1}) is statistically significant.

Our principal component analysis reveals two primary patterns of variability (Fig. 4) from 1920 to 2005. The first is a domainwide pattern that explains 36.6% of the total leaf index variance (Table 1). It is most strongly expressed in the central and western Rockies (Fig. 4a). The time series of this pattern (rPC1) shows a gradual negative trend (earlier spring) starting sometime in the 1950s and an apparent shift toward lower mean values during the mid 1980s. This pattern is essentially the same as the EOF1 pattern in Cayan et al. (2001).

The second pattern explains 16.9% of the variance. It exhibits a dipole spatial pattern with regression coefficients of opposite sign in the northern versus southern part of the domain (Fig. 4b). Positive anomalies in

JOBNAME: JCLI 00#0 2011 PAGE: 6 SESS: 8 OUTPUT: Tue Mar 8 11:16:10 2011 Total No. of Pages: 12
/ams/jcli/0/jcli4069

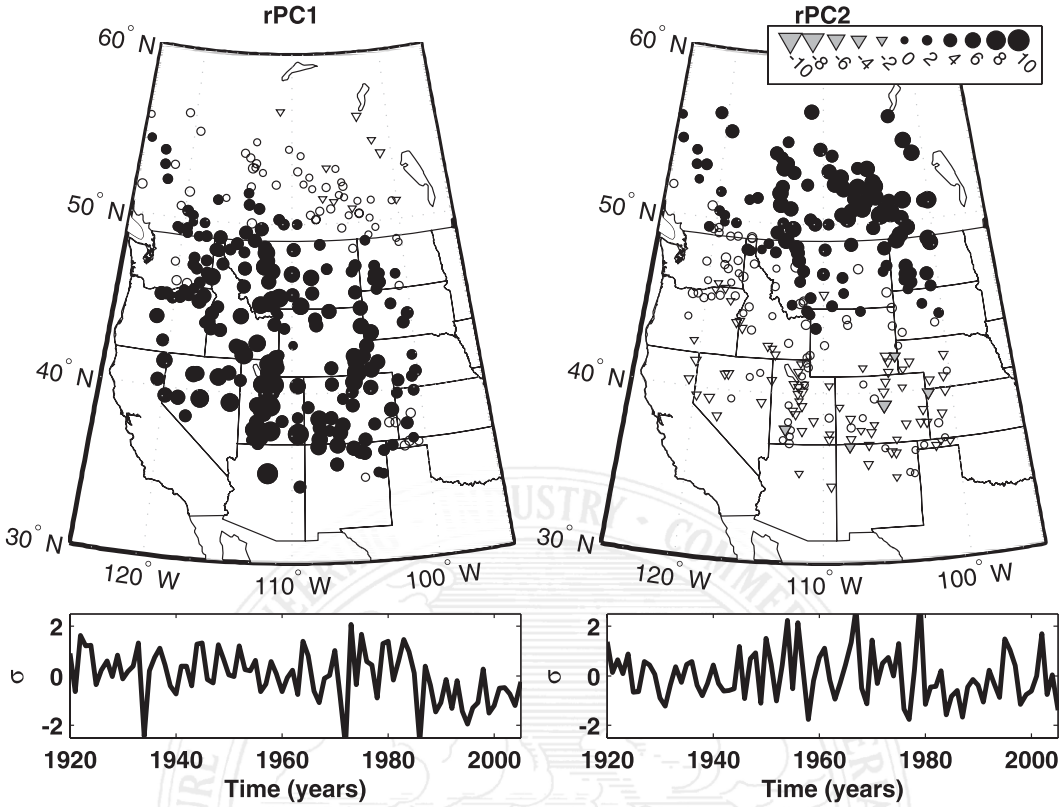

FIG. 4. (top) Patterns and (bottom) time series of the leading two leaf index principal components. Time series are normalized to unit variance and regressed against the raw leaf index data. The size of the regression coefficient therefore corresponds to days of change per unit of standard deviation in the corresponding rPC time series. Shading indicates the regression between the rPC and the raw leaf index time series was significant at the 95% confidence limit.

the time series of rPC2 would correspond to early spring in the south and late spring in the north. The mean of this time series appears to shift toward earlier spring arrival dates during the late 1970s. Again, this spatial pattern is very similar to the lilac EOF2 pattern shown in Cayan et al. (2001).

In March, negative correlations between rPC1 and 300-mb heights (e.g., early spring with high 300-mb heights) occur west of the Aleutian Islands, over much of western North America, and over the subtropical Atlantic Ocean (Fig. 5a). Meanwhile, positive correlations occur over the central North Pacific and northern Atlantic Oceans. Correlations between 300-mb heights and rPC2 in March are not generally significant (Fig. 5b).

During April, significant correlations between rPC1 and 300-mb heights are restricted to a small area of the U.S. Great Plains and northern Alaska (Fig. 5c). Strong negative rPC2 correlations occur over the subtropical Pacific, most of Canada, and part of the eastern Atlantic (Fig. 5d). Regions of positive correlations with rPC2 occur in the North Pacific and the southeastern United States.

Figure 6 shows the regression slopes between normalized versions of the PNA and NAM and the gridded leaf index for March and April. During March, the role of the PNA is significant for most of the domain west of 100°W (Fig. 6a). Regression slopes are negative, indicating that the positive phase of the PNA is associated with early spring, and the negative phase is associated with late spring. Likewise, the March NAM time series regresses (negatively) against the gridded leaf index south of 40°N and west of 108°W, indicating that low-index years are associated with early spring and high-index years with late spring. East of 108°W and north of 45°N there are no significant relationships in Fig. 6a.

TABLE 1. Summary of leaf index variance explained by leading principal component time series (first column) and correlations with the PNA and NAM for March and April (second through fifth columns). Correlations in boldface are significant at the 95% confidence level ($p < 0.05$).

		Correlation			
	Variance	PNA_{Mar}	PNA_{Apr}	NAM_{Mar}	NAM_{Apr}
rPC1	36.59%	−0.04	0.00	**−0.28**	0.03
rPC2	16.94%	−0.08	**−0.37**	0.18	**−0.27**

Journal of Climate (Proof Only)

JOBNAME: JCLI 00#0 2011 PAGE: 7 SESS: 8 OUTPUT: Tue Mar 8 11:16:13 2011 Total No. of Pages: 12
/ams/jcli/0/jcli4069

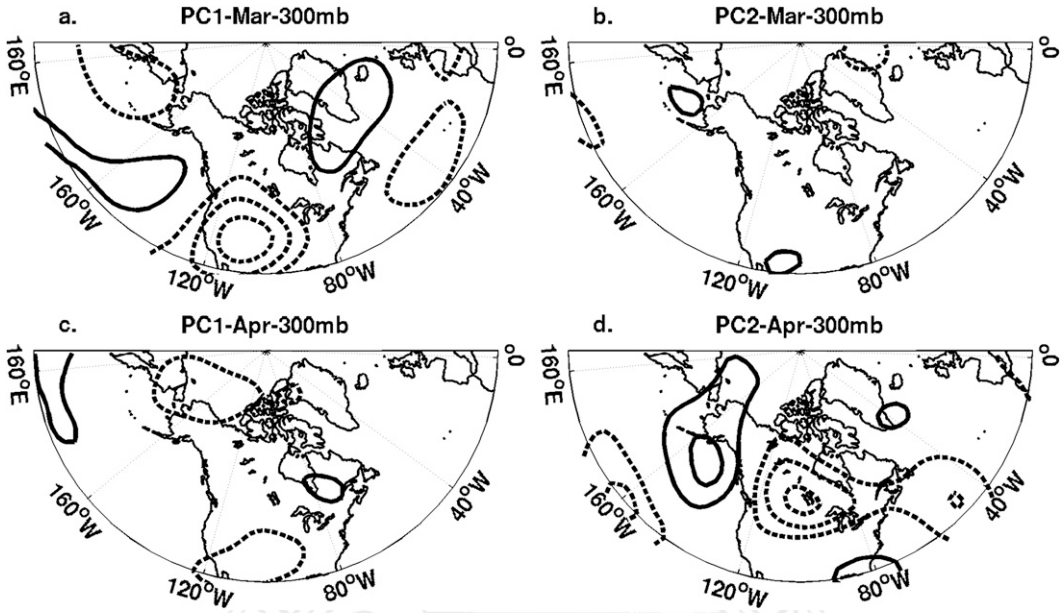

FIG. 5. (a),(b) March and (c),(d) April 300-mb-height correlations between (a),(c) rPC1 and (b),(d) rPC2. Contours are drawn around correlations stronger than ±0.3 at increments of 0.25 (all contoured correlations are significant at the 90% level or higher). Negative correlations (early spring with high 300-mb heights) are contoured in dashed black lines; positive correlations are contoured in solid black lines.

The map of regression slopes in April is quite different (Fig. 6b). Significant slopes are generally not found in latitudes south of 45°N, while grids north of 55°N are significantly (negatively) associated with the PNA. In the Northwest, the state of the NAM in April appears to exert some influence on the timing of spring: positive slopes suggest that high-index years are associated with late spring, and the low-index years are associated with early spring (i.e., the opposite of the relationships in the south). Only a small number of points are significantly related to both the NAM and PNA in March or April.

Figure 6 suggests that western North America may be divided into four regions that respond similarly to the PNA and NAM according to seasonality and geography. These are the Northwest (NW), Canada (CN), the U.S. Southwest (SW), and the southern Great Plains (GP). In the Northwest, the state of the PNA in March exerts a strong influence on the timing of spring, although variability in the NAM in April also plays an important part. In Canada, the March PNA is important in the west but not in the east. This can easily be explained by the mean leaf date values shown in Fig. 1. Stations in the far north and east tend not to experience spring until late April or even May, hence the state of the atmosphere in March is not especially relevant to the timing of leafout, which occurs a month or more later. In the Southwest, the PNA and the NAM exert a similar influence, while in the Great Plains only the NAM seems to influence spring onset.

The results shown here were not especially sensitive to the methodological choices we made. For instance, we have focused our analysis on the first leaf index, but EOF results are very similar if the first bloom index is used instead. We tested the stability of the leaf index spatial patterns shown here by repeating the analysis with two slight modifications. First, we repeated PCA on the gridded leaf index (5° × 5° resolution), and found the leading eigenmodes to be virtually identical to those shown here. Second, we examined the unrotated leading EOFs. This did not impact the spatial pattern of EOF1, but it did emphasize the importance of dipole pattern in EOF2 (as in Cayan et al. 2001, which used unrotated EOFs). We examined composite maps for temperature and 300-mb-height fields to confirm our interpretations of the correlation fields. We also correlated rPC1 and rPC2 with other other geopotential height fields, but these analyses did not substantially alter the patterns shown in Fig. 5.

5. Discussion

The timing of spring, as defined by a well-established phenological model, has been advancing at an average rate of −1.5 days decade^{-1} in WNA from 1950 to 2005 (Fig. 3). Some local trends are near zero and even positive, but these are not significant at the 95% confidence limit (Fig. 3). These estimates are consistent with the

Journal of Climate (Proof Only)

JOBNAME: JCLI 00#0 2011 PAGE: 8 SESS: 8 OUTPUT: Tue Mar 8 11:16:18 2011 Total No. of Pages: 12
/ams/jcli/0/jcli4069

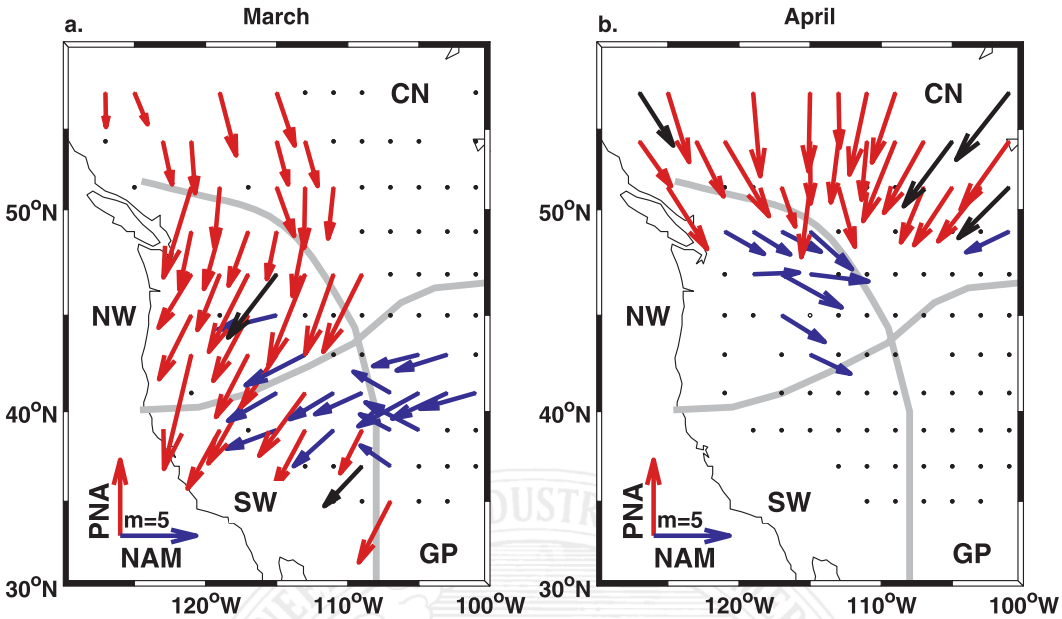

FIG. 6. Regression slopes between each leaf index time series and normalized versions of the NAM and PNA for (a) March and (b) April. Vectors indicate that the regression slope is significant ($p < 0.05$) for at least one of the two modes: red indicates a significant contribution from the PNA, blue indicates a significant NAM contribution, and black indicates the contribution of both modes is significant. Regression coefficients between each individual grid point and the PNA are shown along the y axis (arrows). Negative values (arrows pointing downward) associate early spring with the positive phase of the PNA. Regression coefficients between each grid point and the NAM are shown along the x axis. Positive slopes, indicated by rightward-pointing arrows, relate low-index years to early spring and high-index years to late spring. Negative slopes indicate the opposite relationship. Arrow length indicates the magnitude of the slope in days per standard deviation of PNA or NAM variability. The keys in the bottom left corner of (a) and (b) show the length of arrows that would correspond to 5 days of spring onset variability per one standard deviation of PNA or NAM variability. Dots indicate grids where no significant correlations were found; land areas without dots indicate grids where there were either no available stations (e.g., the Pacific coast and Northern Mexico). AU4

results of Schwartz et al. (2006), which found a hemispheric trend in leaf index of −1.2 days decade^{-1} from 1955 to 2002 and individual station trends in the WNA region between +0.3 and −3.0 days decade^{-1} from 1961 to 2000. Our estimates are also well within the hemispheric averages of phenological observations described by Parmesan (2006) but slightly more negative. One-third of the regionwide trend (−0.5 day decade^{-1}) may be explained by trends in the PNA and NAM, but the remaining trend is still statistically significant. Abatzoglou (2011) showed a similar influence of the PNA on secular trends in the elevation of the freezing level, decreases in the percentage of precipitation falling as snow, and increases in snowmelt across the western United States. As in our study, significant trends remained when the PNA influence was removed.

Two patterns of variability explain roughly 50% of the total variance in the onset date of spring from 1920 to 2005. Similar patterns were identified in an earlier study of (independent) phenological observations (Cayan et al. 2001), which implies that the patterns reflect robust regional responses to interannual climate variability. Figure 5 supports this interpretation, suggesting that circulation anomalies in the atmosphere help determine the ultimate arrival date of spring. However, the rPC time series do not correspond one-to-one with known modes of atmospheric variability, such as the PNA and NAM (Table 1). Rather, leaf index values for individual grid points respond to both modes of Northern Hemisphere atmospheric circulation according to geography and seasonality (Fig. 6).

To further explore the mechanisms by which atmospheric variability modulates spring arrival date, we return to the predictor variables used to calculate the leaf index. We calculate the number of high-energy synoptic events (defined as the rapid accumulation of warmth over a short period of time in Schwartz and Marotz 1988) that occur in daily NCEP reanalysis data during different configurations of the monthly NAM and PNA time series (Figs. 7 and 8). We focus on this variable because it is sensitive to the position of spring storm tracks, which are expected to vary in response to the state of the Northern Hemisphere

Journal of Climate (Proof Only)

JOBNAME: JCLI 00#0 2011 PAGE: 9 SESS: 8 OUTPUT: Tue Mar 8 11:16:18 2011 Total No. of Pages: 12
/ams/jcli/0/jcli4069

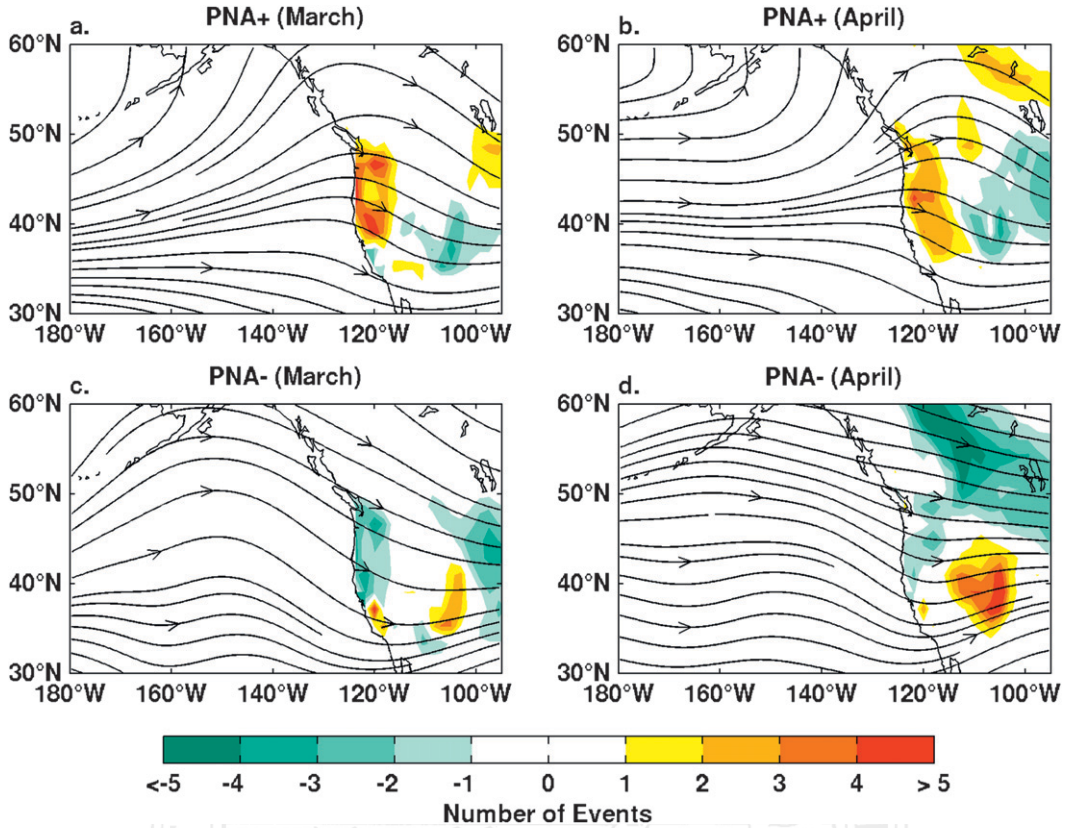

FIG. 7. Composite maps of anomalous numbers of "warm events" (colors) and 300-mb wind (streamlines) for the (a),(b) positive ($>1\sigma$) and (c),(d) negative ($<-1\sigma$) phases of the PNA during (a),(c) March and (b),(d) April. A warm event is defined by a rapid rise in 3-day AGDH. The monthly warm event mean was removed prior to calculating the composites, so that each map represents the average number of events above or below the long-term mean during the different phases of the PNA.

modes of variability (e.g., Quadrelli and Wallace 2002; McAfee and Russell 2008).

The positive phase of the PNA is associated with a deepened Aleutian low and a warm ridge over western North America (Wallace and Gutzler 1981). Accordingly, the number of warm events in the Pacific Northwest is anomalously high during March (Fig. 7a) and April (Fig. 7b). During the PNA's negative phase, a weaker Aleutian low and a trough over WNA steer cold polar air masses along the West Coast of North America (Wallace and Gutzler 1981). This can be seen in the wind fields in Figs. 7c and 7d and in the anomalously low number of warm events during those years. These results help explain, in part, the negative relationship between the leaf index and the PNA.

We observe that when the NAM is in its positive phase during March, there are a greater number of warm events throughout most of the western United States (Fig. 8a). Positive phases of the NAM correspond to a northward displacement of winter storm tracks and fewer outbreaks of cold air (Thompson and Wallace 2001, 1998; Thompson et al. 2000), which allows warm air masses from the south to be advected into the Southwest and the Great Plains, producing earlier springs. Late springs, on the other hand, may be caused by enhanced meridional flow during the negative phase of the NAM. At these times, outbreaks of cold air tend to be more common, especially east of the Rocky Mountains (Thompson and Wallace 2001), which reduces the number of warm events. Figure 8c connects this tendency to the Great Plains regressions shown in Fig. 6a: the decrease in warm events during the NAM's negative phase works to prolong spring.

The results in Fig. 8 might also help explain the abrupt nature of the trend in rPC1, which shifts toward earlier dates around the mid-1980s. A similar shift is also present in the study of Cayan et al. (2001), which was based on the raw lilac and honeysuckle phenological observations. This is important to note because it means that the shift is not an artifact of the model and that the actual plant response may be more pronounced than the climate data alone would suggest. During the 1980s, there was also a shift in the polarity of the NAM during March toward

Journal of Climate (Proof Only)

JOBNAME: JCLI 00#0 2011 PAGE: 10 SESS: 8 OUTPUT: Tue Mar 8 11:16:27 2011 Total No. of Pages: 12
/ams/jcli/0/jcli4069

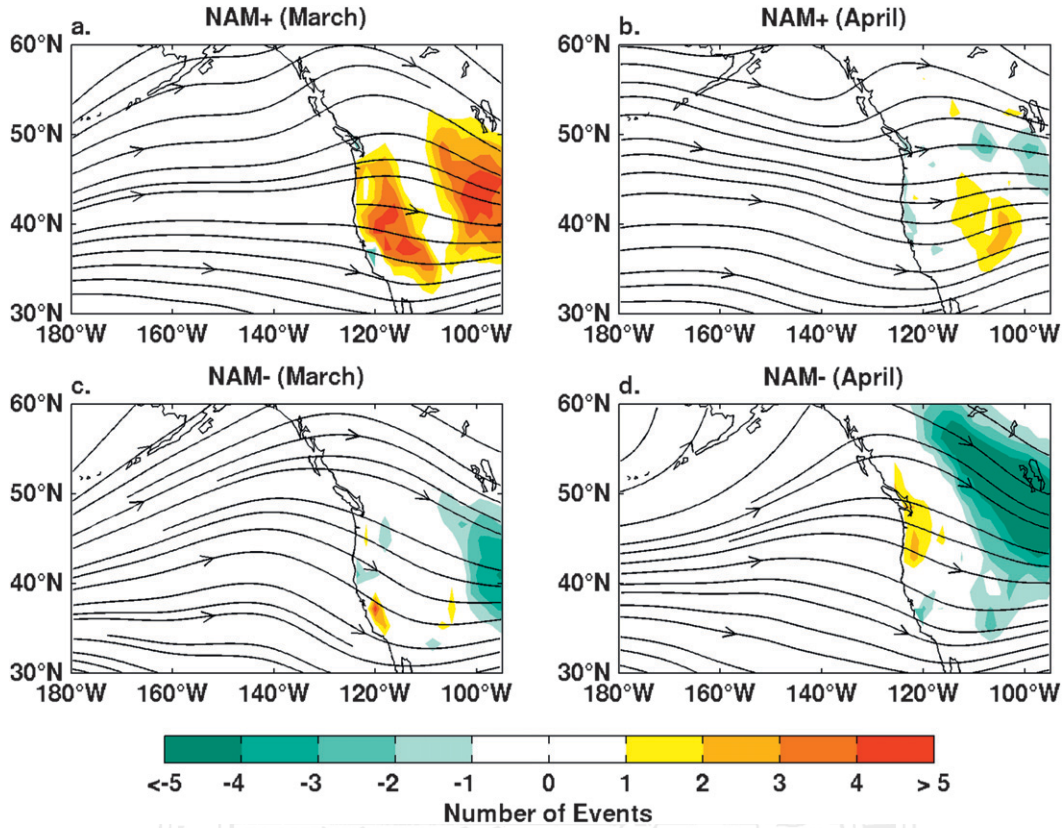

FIG. 8. As in Fig. 7, but for the NAM.

higher index values (Thompson and Wallace 1998; McAfee and Russell 2008). A change in this direction would favor earlier warm air mass intrusions and thus earlier springs.

6. Conclusions

We have shown that, from 1950 to 2005, there is a trend in the WNA regionwide average leaf index of about −1.5 days decade^{-1}. One-third (−0.5 day decade^{-1}) of this trend can be explained by trends in the NAM and PNA, but the remaining trend is still statistically significant.

Roughly half of the variance in spring onset dates from 1920 to 2005 in western North America can be explained by two patterns of variability. The first is a domainwide pattern (Fig. 4a) linked to circulation anomalies during March (Fig. 5). It is weakly (but significantly) correlated with the northern annular mode in March. The second pattern exhibits a north–south dipole structure (Fig. 4b), but it reflects primarily a high-latitude response to circulation patterns during April (Fig. 5). It is correlated with the April PNA such that negative anomalies in the PNA time series correspond to late spring in the north and early spring in the south (and positive anomalies in the PNA correspond to early spring in the north and late spring in the south).

Analysis of gridded leaf index time series (Fig. 6) reveals regional and seasonal sensitivities to both the PNA and the NAM. In the Northwest, the state of the March PNA influences spring arrival by bringing a greater number of warm days to the region during the positive phase, whereas the negative phase of the NAM in April can delay spring. The March PNA is also important to the timing of spring onset in western, but not eastern, Canada. In April, the PNA influences spring arrival throughout northern latitudes, whereas southern latitudes are not sensitive to April conditions because spring has already occurred by that time. In the Southwest, early spring is associated with a northward shift in storm tracks during March, which allows more warm air into the region earlier. This can occur from either the negative state of the PNA or the positive state of the NAM. A similar mechanism influences early spring in the Great Plains; during the NAM's low-index phase, outbursts of cold air delay spring in the region.

Although the indices used here have been computed from station data, they require only daily T_{min} and T_{max} values as input, which could be obtained from reanalysis or global climate model data. Future studies could therefore

Journal of Climate (Proof Only)

JOBNAME: JCLI 00#0 2011 PAGE: 11 SESS: 8 OUTPUT: Tue Mar 8 11:16:40 2011 Total No. of Pages: 12
/ams/jcli/0/jcli4069

use climate-modeling experiments to better understand the atmospheric dynamics of spring onset. Future studies could also examine how the full suite of spring index variables (Schwartz et al. 2006) responds to interannual and decadal climate variability at the hemispheric scale. Such an analysis would, in turn, improve assessments of ecological and hydrological impacts of climate change. Future analyses could also inform strategic development of the USA National Phenology Network (www.usanpn.org). Finally, if global climate models can be used to project the mean state of the PNA and NAM on decadal time scales, knowledge of how the PNA and the NAM relate to the timing of spring across WNA could inform long-term natural resource management, improving the prospects for successful adaptation strategies under climate change.

Acknowledgments. We thank C. Castro, J. E. Cole, G. McCabe, S. McAfee, J. Russell, C. Woodhouse, and J. L. Weiss for helpful comments. We also thank B. Cook, L. Wolkovitch, and the National Center for Ecological Analysis and Synthesis. This research benefited from feedback at the PACLIM 2009 Conference, with travel support provided by S. Starratt and the PACLIM 2009 organizers as well as the Institute of the Environment, University of Arizona. TA was supported by an NSF GRFP and NOAA CCDD (NA07OAR4310054), and AM was supported by the DOE GREF and SfAZ GRFP. Any use of trade, product, or firm names is for descriptive purposes only and does not imply endorsement by the U.S. Government.

REFERENCES

Abatzoglou, J. T., 2011: Influence of the PNA on declining mountain snowpack in the western United States. *Int. J. Climatol.,* doi:10.1002/joc.2137, in press. AU1

——, and K. T. Redmond, 2007: Asymmetry between trends in spring and autumn temperature and circulation regimes over western North America. *Geophys. Res. Lett.,* **34,** L18808, doi:10.1029/2007GL030891.

Alley, W. M., 1984: The Palmer drought severity index—Limitations and assumptions. *J. Climate Appl. Meteor.,* **23,** 1100–1109.

Barnett, T. P., and Coauthors, 2008: Human-induced changes in the hydrology of the western United States. *Science,* **319,** 1080–1083.

Betancourt, J., M. Schwartz, D. Breshears, D. Cayan, M. Dettinger, D. Inouye, E. Post, and B. Reed, 2005: Implementing a U.S. National Phenology Network. *Eos, Trans. Amer. Geophys. Union,* **86,** 51, doi:10.1029/2005EO510005.

Bonfils, C., and Coauthors, 2008: Detection and attribution of temperature changes in the mountainous western United States. *J. Climate,* **21,** 6404–6424.

Brown, J., S. Li, and N. Bhagabati, 1999: Long-term trend toward earlier breeding in an American bird: A response to global warming? *Proc. Natl. Acad. Sci. USA,* **96,** 5565–5569.

Caprio, J. M., 1993: Western regional phenological summary of information on honeysuckle and lilac first bloom phase covering the period 1956–1991. Montana Agricultural Experiment Station State Climate Center Circular, No. 3, 92 pp.

Cayan, D. R., S. A. Kammerdiener, M. D. Dettinger, J. M. Caprio, and D. H. Peterson, 2001: Changes in the onset of spring in the western United States. *Bull. Amer. Meteor. Soc.,* **82,** 399–415.

Das, T., and Coauthors, 2009: Structure and detectability of trends in hydrological measures over the western United States. *J. Hydrometeor.,* **10,** 871–892.

de Beurs, K. M., and G. M. Henebry, 2008: Northern annular mode effects on the land surface phenologies of northern Eurasia. *J. Climate,* **21,** 4257–4279.

Forister, M., and A. Shapiro, 2003: Climatic trends and advancing spring flight of butterflies in lowland California. *Global Change Biol.,* **9,** 1130–1135.

Guttman, N. B., 1999: Accepting the standardized precipitation index: A calculation algorithm. *J. Amer. Water Resour. Assoc.,* **35,** 311–322.

Hamlet, A. F., P. W. Mote, M. P. Clark, and D. P. Lettenmaier, 2007: Twentieth-century trends in runoff, evapotranspiration, and soil moisture in the western United States. *J. Climate,* **20,** 1468–1486.

Hidalgo, H. G., and Coauthors, 2009: Detection and attribution of streamflow timing changes to climate change in the western United States. *J. Climate,* **22,** 3838–3855.

Inouye, D. W., 2008: Effects of climate change on phenology, frost damage, and floral abundance of montane wildflowers. *Ecology,* **89,** 353–362.

Johnson, R. H., P. E. Ciesielski, B. D. McNoldy, P. J. Rogers, and R. K. Taft, 2007: Multiscale variability of the flow during the North American Monsoon Experiment. *J. Climate,* **20,** 1628–1648.

Kalnay, E., and Coauthors, 1996: The NCEP/NCAR 40-Year Reanalysis Project. *Bull. Amer. Meteor. Soc.,* **77,** 437–471.

Karl, T. R., J. M. Melillo, and T. C. Peterson, Eds., 2009: *Global Climate Change Impacts in the United States.* Cambridge University Press, 188 pp.

Littell, J. S., D. McKenzie, D. L. Peterson, and A. L. Westerling, 2009: Climate and wildfire area burned in western U. S. ecoprovinces, 1916–2003. *Ecol. Appl.,* **19,** 1003–1021.

Lorenz, D. J., and E. T. DeWeaver, 2007: Tropopause height and zonal wind response to global warming in the IPCC scenario integrations. *J. Geophys. Res.,* **112,** D10119, doi:10.1029/2006JD008087. AU2

McAfee, S. A., and J. L. Russell, 2008: Northern annular mode impact on spring climate in the western United States. *Geophys. Res. Lett.,* **35,** L17701, doi:10.1029/2008GL034828.

McCabe, G., and M. Clark, 2005: Trends and variability in snowmelt runoff in the western United States. *J. Hydrometeor.,* **6,** 476–482.

McKenzie, D., Z. Gedalof, D. Peterson, and P. Mote, 2004: Climatic change, wildfire, and conservation. *Conserv. Biol.,* **18,** 890–902.

Moore, R. D., S. W. Fleming, B. Menounos, R. Wheate, A. Fountain, K. Stahl, K. Holm, and M. Jakob, 2009: Glacier change in western North America: influences on hydrology, geomorphic hazards and water quality. *Hydrol. Processes,* **23,** 42–61.

Mote, P., A. Hamlet, M. Clark, and D. Lettenmaier, 2005: Declining mountain snowpack in western North America. *Bull. Amer. Meteor. Soc.,* **86,** 39–49.

Palmer, W. C., 1965: Meteorological drought. U.S. Department of Commerce, Research Paper 45, 65 pp.

Journal of Climate (Proof Only)

JOBNAME: JCLI 00#0 2011 PAGE: 12 SESS: 8 OUTPUT: Tue Mar 8 11:16:40 2011 Total No. of Pages: 12
/ams/jcli/0/jcli4069

Parmesan, C., 2006: Ecological and evolutionary responses to recent climate change. *Annu. Rev. Ecol. Evol. Syst.,* **37,** 637–669, doi:10.1146/annurev.ecolsys.37.091305.110100.

Pierce, D. W., and Coauthors, 2008: Attribution of declining western U.S. snowpack to human effects. *J. Climate,* **21,** 6425–6444.

Preisendorfer, R. W., C. D. Mobley, and T. P. Barnett, 1988: The principal discriminant method of prediction—Theory and evaluation. *J. Geophys. Res.,* **93,** 10 815–10 830.

Qian, T. T., A. Dai, K. E. Trenberth, and K. W. Oleson, 2006: Simulation of global land surface conditions from 1948 to 2004. Part I: Forcing data and evaluations. *J. Hydrometeor.,* **7,** 953–975.

Quadrelli, R., and J. M. Wallace, 2002: Dependence of the structure of the Northern Hemisphere annular mode on the polarity of ENSO. *Geophys. Res. Lett.,* **29,** 2132, doi:10.1029/2002GL015807.

——, and ——, 2004: A simplified linear framework for interpreting patterns of Northern Hemisphere wintertime climate variability. *J. Climate,* **17,** 3728–3744.

Schwartz, M. D., 1985: The advance of phenological spring across eastern and central North America. Ph.D. thesis, University of Kansas, XX pp.

AU3

——, 1992: Phenology and springtime surface layer change. *Mon. Wea. Rev.,* **120,** 2570–2578.

——, and G. A. Marotz, 1986: An approach to examining regional atmosphere plant interactions with phenological data. *J. Biogeogr.,* **13,** 551–560.

——, and ——, 1988: Synoptic events and spring phenology. *Phys. Geogr.,* **9,** 151–161.

——, and T. R. Karl, 1990: Spring phenology—Nature's experiment to detect the effect of greenup on surface maximum temperatures. *Mon. Wea. Rev.,* **118,** 883–890.

——, and B. E. Reiter, 2000: Changes in North American spring. *Int. J. Climatol.,* **20,** 929–932.

——, and X. Chen, 2002: Examining the onset of spring in China. *Climate Res.,* **21,** 157–164.

——, G. J. Carbone, G. L. Reighard, and W. R. Okie, 1997: A model to predict peach phenology and maturity using meteorological variables. *HortScience,* **32,** 213–216.

——, R. Ahas, and A. Aasa, 2006: Onset of spring starting earlier across the Northern Hemisphere. *Global Change Biol.,* **12,** 343–351.

Solomon, S., D. Qin, M. Manning, M. Marquis, K. Averyt, M. M. B. Tignor, H. L. Miller, and Z. Chen, Eds., 2007: *Climate Change 2007: The Physical Science Basis*. Cambridge University Press, 996 pp.

Stenseth, N., A. Mysterud, G. Ottersen, J. Hurrell, K. Chan, and M. Lima, 2002: Ecological effects of climate fluctuations. *Science,* **297,** 1292–1296.

Stewart, I. T., D. R. Cayan, and M. D. Dettinger, 2005: Changes toward earlier streamflow timing across western North America. *J. Climate,* **18,** 1136–1155.

Thompson, D. W. J., and J. M. Wallace, 1998: The Arctic oscillation signature in the wintertime geopotential height and temperature fields. *Geophys. Res. Lett.,* **25,** 1297–1300.

——, and ——, 2000: Annular modes in the extratropical circulation. Part I: Month-to-month variability. *J. Climate,* **13,** 1000–1016.

——, and ——, 2001: Regional climate impacts of the Northern Hemisphere annular mode. *Science,* **293,** 85–89.

——, ——, and G. C. Hegerl, 2000: Annular modes in the extratropical circulation. Part II: Trends. *J. Climate,* **13,** 1018–1036.

Wallace, J. M., and D. S. Gutzler, 1981: Teleconnections in the geopotential height field during the Northern Hemisphere winter. *Mon. Wea. Rev.,* **109,** 784–812.

Westerling, A. L., H. G. Hidalgo, D. R. Cayan, and T. W. Swetnam, 2006: Warming and earlier spring increase western U.S. forest wildfire activity. *Science,* **313,** 940–943.

Zhang, Y., J. Wallace, and D. S. Battisti, 1997: ENSO-like interdecadal variability: 1900–93. *J. Climate,* **10,** 1004–1020.

Journal of Climate (Proof Only)